HHS Public Access

Author manuscript

Sci Transl Med. Author manuscript; available in PMC 2016 March 09.

Published in final edited form as:

Sci Transl Med. 2015 May 6; 7(286): 286ra67. doi:10.1126/scitranslmed.aaa1652.

Identification of a plant isoflavonoid that causes biliary atresia

Kristin Lorent[1,*], **Weilong Gong**[1,*], **Kyung A. Koo**[2,*], **Orith Waisbourd-Zinman**[3,4], **Sara Karjoo**[3], **Xiao Zhao**[1], **Ian Sealy**[5], **Ross N. Kettleborough**[5], **Derek L. Stemple**[5], **Peter A. Windsor**[6], **Stephen J. Whittaker**[7], **John R. Porter**[2], **Rebecca G. Wells**[1,8,†], and **Michael Pack**[1,9,†]

[1]Department of Medicine, Perelman School of Medicine, University of Pennsylvania, Philadelphia, PA 19104, USA.

[2]Department of Biological Sciences, University of the Sciences, Philadelphia, PA 19104, USA.

[3]Division of Pediatric Gastroenterology, Hepatology, and Nutrition, The Children's Hospital of Philadelphia, Philadelphia, PA 19104, USA.

[4]Sackler Faculty of Medicine, Tel-Aviv University, Tel-Aviv, Israel.

[5]Wellcome Trust Sanger Institute, Wellcome Trust Genome Campus, Hinxton, Cambridge CB10 1SA, UK.

[6]Faculty of Veterinary Science, University of Sydney, Camden, New South Wales 2570, Australia.

[7]Hume Livestock Health and Pest Authority, Albury, New South Wales 2640, Australia.

[†]Corresponding author. rgwells@mail.med.upenn.edu (R.G.W.); mpack@mail.med.upenn.edu (M.P.).
[*]These authors contributed equally to this work.

SUPPLEMENTARY MATERIALS

www.sciencetranslationalmedicine.org/cgi/content/full/7/286/286ra67/DC1

Fig. S1. Swallowing function of biliatresone-treated larvae.
Fig. S2. Scheme for biliatresone isolation.
Fig. S3. Biliatresone-mediated biliary secretion defect.
Fig. S4. Biliatresone dose response in zebrafish.
Fig. S5. Biliatresone biliary secretion dose response.
Fig. S6. Macrophages not required for biliatresone toxicity.
Fig. S7. Biliatresone treatment during embryogenesis.
Fig. S8. No effect of biliatresone on digestive epithelia.
Fig. S9. Bile flow requirement for biliatresone toxicity.
Fig. S10. Zebrafish *ductbend* mutants.
Fig. S11. *ductbend* biliatresone sensitivity.
Fig. S12. *ductbend* candidate gene expression.
Fig. S13. Biliatresone-induced defects of cholangiocyte cilia and microtubules.
Fig. S14. Dose-dependent loss of cholangiocyte microtubules with biliatresone treatment.
Fig. S15. Effects of biliatresone on hepatocytes.
Fig. S16. Lack of effect of isoflavanone-3 on mammalian cholangiocyte spheroids.
Fig. S17. Effects of betavulgarin on mammalian cholangiocyte spheroids.
Table S1. Biliatresone toxicity in DAPT-treated larvae.
Movie S1. Biliary anatomy of a wild-type larva.
Movie S2. Biliary anatomy of a toxin-treated wild-type larva.

Author contributions: P.A.W. and S.J.W. helped procure *Dysphania* plants and diagnosed biliary atresia in livestock. K.L., W.G., K.A.K., O.W.-Z., S.K., X.Z., I.S., R.N.K., D.L.S., J.R.P., R.G.W., and M.P. performed experiments. K.L., K.A.K., J.R.P., R.G.W., and M.P. wrote the manuscript.

Competing interests: The authors declare that they have no competing interests.

Data and materials availability: Synthetic biliatresone will be provided to academic researchers when available.

[8]Department of Pathology and Laboratory Medicine, Perelman School of Medicine, University of Pennsylvania, Philadelphia, PA 19104, USA.

[9]Cell and Developmental Biology, Perelman School of Medicine, University of Pennsylvania, Philadelphia, PA 19104, USA.

Abstract

Biliary atresia (BA) is a rapidly progressive and destructive fibrotic disorder of unknown etiology affecting the extrahepatic biliary tree of neonates. Epidemiological studies suggest that an environmental factor, such as a virus or toxin, is the cause of the disease, although none have been definitively established. Several naturally occurring outbreaks of BA in Australian livestock have been associated with the ingestion of unusual plants by pregnant animals during drought conditions. We used a biliary secretion assay in zebrafish to isolate a previously undescribed isoflavonoid, biliatresone, from *Dysphania* species implicated in a recent BA outbreak. This compound caused selective destruction of the extrahepatic, but not intrahepatic, biliary system of larval zebrafish. A mutation that enhanced biliatresone toxicity mapped to a region of the zebrafish genome that has conserved synteny with an established human BA susceptibility locus. The toxin also caused loss of cilia in neonatal mouse extrahepatic cholangiocytes in culture and disrupted cell polarity and monolayer integrity in cholangiocyte spheroids. Together, these findings provide direct evidence that BA could be initiated by perinatal exposure to an environmental toxin.

INTRODUCTION

Biliary atresia (BA) is a disorder affecting neonates that is characterized by rapidly progressive fibrotic damage to the extrahepatic biliary tree. Its etiology is currently unknown. Although BA is a rare disorder (with an incidence ranging from 1:8000 to 1:15,000 live births), it is the most common indication for liver transplant in the pediatric population (1). Patients present as neonates with obstructive jaundice and develop rapidly progressive biliary fibrosis despite surgical correction of the extrahepatic atresia. Many infants have liver cirrhosis at the time of diagnosis. About 10% of BA patients have associated developmental abnormalities, such as situs inversus and polysplenia, although in most the biliary disease is an isolated finding. The timing of biliary injury in isolated BA is not known; however, a recent study suggests that the injury could occur prenatally (2). Neither form of BA displays Mendelian inheritance, and most twin studies have shown nonconcordance, thus arguing against a single genetic determinant. Genome-wide association studies (GWAS) have led to identification of potential BA susceptibility loci on several different chromosomes, and a recent study suggested an association between BA risk and specific mitochondrial DNA haplogroups (3–6). Unfortunately, none of the affected genes within these regions have been identified.

Nonrandom clustering of BA cases in space and time suggests an environmental cause, either infectious or toxic (7–9). Supporting the former, infection of neonatal (up to 72 hours old) mice with rhesus rotavirus (RRV) yields a BA-like syndrome that recapitulates many features of human BA, particularly the immunological events associated with duct atresia.

There is considerable overlap in the immune cell populations surrounding portal tracts and the extrahepatic ducts in RRV-infected mice and BA patients; however, no definitive evidence of rotavirus infection has been found in human BA (10, 11). Perinatal infection with cytomegalovirus (CMV) has been associated with some cases of isolated BA (11), although it remains controversial whether CMV infection is causative or acquired secondarily. A role for reovirus has also been suggested, but the supporting data are inconclusive (12).

Naturally occurring outbreaks of BA occurred in herds of sheep and, in one case, cows of mixed genetic stock in New South Wales, Australia, in 1964, 1988, 2007, and 2013, affecting 14 to 100%of newborn animals but sparing their mothers and other adult animals (13, 14). In each of these years, there was severe drought, and animals, including pregnant dams, were grazed on lands that are normally under water. Common to the flora of these atypical pastures were chenopods in the genus *Dysphania*, suggesting a toxic cause of the BA. The 2007 drought persisted through 2008, enabling us to harvest *Dysphania* species plants from a pasture implicated in the 2007 episode. In an effort to identify biliary toxins, we carried out sequential fractionation of the plants, guided by a zebrafish bioassay. We report here the isolation of a previously uncharacterized toxin that causes selective atresia of the extrahepatic biliary tree in zebrafish. Supporting studies in zebrafish and mouse biliary cells suggest potential links between toxin-induced biliary injury and human BA.

RESULTS

Isolation and biochemical characterization of biliatresone

We harvested 3 kg of *Dysphania* species plants in 2008.A single plant analyzed at the Royal Botanic Gardens in Melbourne was identified as *Dysphania littoralis*, although it is likely that we harvested a mixed population of *D. littoralis* and *Dysphania glomulifera* ssp. *glomulifera* because these species often grow together and can be differentiated only microscopically. Plants were frozen immediately after collection and shipped to the United States. A portion of the plant material was initially extracted with methylene chloride/ methanol (1:1, v/v). The resulting fraction was partitioned to petroleum ether and methanol, with aqueous extraction of the remaining plant biomass, yielding three crude fractions containing compounds over a wide range of polarities.

We exposed zebrafish larvae at 5 days postfertilization (dpf) (when the biliary system is fully formed) to the initial three plant fractions (30 μg/ml) for 72 hours. Larvae were then allowed to ingest the fluorescent lipid reporter PED-6 (a quenched phospholipid) and Bodipy-C5 and Bodipy-C16 (short- and long-chain fatty acids, respectively) from their aqueous medium (15). Exposure of larvae to the methanolic fraction (30 μg/ml) resulted in markedly reduced fluorescence in the gallbladders and intestines in all of the larvae surviving treatment (n = 25 surviving larvae of 50 treated; as indicated in Fig. 1, A and B). In control experiments, neither this fraction nor purified toxin prevented fish from ingesting the lipid reporter from the aqueous medium (fig. S1). Together, these findings pointed to the presence of a biliary-specific toxin in the methanolic fraction.

To purify the toxin, we performed 10 rounds of reiterative fractionation using the zebrafish bioassay (95 individual fractions, each tested in triplicate; fig. S2). Ultimately, we isolated and structurally characterized four pure compounds (Fig. 1C) from a complex active fraction and determined that a single compound, the previously uncharacterized isochalcone, biliatresone (4-methoxy-*seco*-betavulgarin), exhibited biliary toxicity in the zebrafish bioassay, whereas the other three compounds were inactive. The active toxin had a yield of 1.84% of the dry weight of the plant. The three compounds without biliary or other toxicity in the zebrafish assay were all structurally similar and likely a part of the same biosynthetic pathway that includes biliatresone. Two are previously uncharacterized compounds, an isoflavanone and a pterocarpan (Fig. 1C, compounds **3** and **4**), but one was the previously described isoflavonoid, betavulgarin (Fig. 1C, compound **2**), which is found in medicinal herbs and plants, including *Beta vulgaris*, a species with several edible varieties, including chard, table beet, and sugar beet (16, 17). Screening of other subfractions with the zebrafish assay showed that these fractions caused cardiac defects and/or lethality, suggesting that there are likely additional toxic compounds but without the specific biliary effects reported here. Purified biliatresone had comparable effects on the excretion of short- and long-chain fatty acid reporters, which are absorbed through different mechanisms, further arguing that it blocked bile secretion, rather than absorption of the lipid reporters (fig. S3).

Selective extrahepatic biliary toxicity of biliatresone

To characterize the effects of biliatresone on extrahepatic biliary morphology, we immunostained larvae treated with escalating doses of the toxin using a monoclonal antibody that recognizes zebrafish biliary and gallbladder epithelial cells, and then we analyzed them using confocal microscopy. Larvae treated at 5 dpf with low doses of biliatresone [0.0625 μg/ml (0.2 μM) and 0.125 μg/ml (0.4 μM)] showed only subtle gallbladder defects (fig. S4), whereas larvae treated with higher doses had pronounced morphological defects of the gallbladder and extrahepatic ducts (Fig. 1, D to G, and fig. S4). Confocal microscopy allowed observation of altered morphology of the gallbladder epithelium in 5 dpf larvae treated with the toxin (0.25 μg/ml, 0.8 μM) (fig. S4); the gallbladder was severely dysmorphic, and the extrahepatic bile ducts were difficult to recognize in larvae treated with higher doses of toxin [0.5 μg/ml (1.6 μM) and 1.0 μg/ml (3.2 μM); Fig. 1, D to G, fig. S4, and movie S1 for untreated control larva and movie S2 for biliatresone-treated larva]. In general, gallbladder epithelial cells appeared more sensitive to lower doses of the toxin than did epithelial cells lining the extrahepatic ducts (fig. S4). Similar dose responsiveness to biliatresone was detected using a biliary secretion screening assay to measure gallbladder fluorescence (fig. S5).

The intrahepatic ductal system, as visualized with confocal microscopy, was preserved in all treated larvae (Fig. 1, D to G, figs. S4 and S6, and movies S1 and S2), thus indicating that the toxin specifically targeted cholangiocytes within the extrahepatic ducts and gallbladder. Larvae that were exposed to biliatresone beginning at 6 hours postfertilization (hpf) and 24 hpf (as opposed to 5 dpf) had normal morphology at 5 dpf, other than morphological changes typical of a developmental delay (fig. S7). Cardiac and gut looping were not affected by these earlier treatments, thus indicating that the toxin did not alter organ chirality (n = 4 groups of 24 larvae treated with biliatresone at doses of 0.0625, 0.125, 0.25, and 0.5

μg/ml from6 to 36 hpf, all with normal cardiac and gut chirality). Identical extrahepatic bile duct effects of the toxin were seen in older larvae (treatment initiated at 8 and 13 dpf) as in 5 dpf larvae, albeit at lower doses, suggesting greater sensitivity to the toxin at these developmental stages (fig. S4, H and I versus C and D). Larvae exposed to doses of biliatresone that cause severe gallbladder and extrahepatic duct defects at 5 dpf (1 μg/ml for 72 hours) did not survive longer than 12 dpf, even when the toxin was removed from the aqueous medium at 8 dpf. A limited quantity of purified toxin has prevented us from characterizing the activity of biliatresone in adult fish or mammalian models.

Histological analyses confirmed that biliatresone is an extrahepatic biliary toxin. All toxin-treated larvae with altered extrahepatic morphology on confocal microscopy had severe morphological defects of the extrahepatic bile duct and gallbladder in histological sections (Fig. 2, A and B; $n = 10$ larvae examined). Histological sections through the liver showed no change in the appearance of hepatocytes, sinusoidal endothelia, or intestinal epithelia in biliatresone-treated larvae (Fig. 2, A to D, and fig. S8). Because of their small size, the intrahepatic bile ducts are not visible in histological sections (18); however, their morphology was normal in the confocal projections of immunostained larvae (Fig. 1, figs. S4 and S6, and movie S1). There was no obvious effect of biliatresone on hepatic synthetic function, as evidenced by normal liver fluorescence in transgenic larvae that express red fluorescent protein (RFP) under the control of a *liver fatty acid binding protein* promoter fragment [*Tg*(*lfabp:RFP*)] (Fig. 2, E to H).

Innate immune cell response to biliatresone

In some cases of human BA, a prominent inflammatory cell infiltrate consisting of T helper and cytotoxic T cells and macrophages is detected within and surrounding the intrahepatic ducts, and less frequently the extrahepatic ducts at the time of diagnosis (11, 19, 20). Whether this arises purely as a response to cholangiocyte injury or involves direct activation of the innate and/or adaptive immune systems is not known. An inflammatory infiltrate is also present in livers of affected lambs with the *Dysphania* BA syndrome at late time points, and in the RRV BA model, in which roles for lymphocytes [T helper, T cytotoxic, natural killer (NK), regulatory T cells, and B cells], dendritic cells, and innate immune cells (macrophages and granulocytes) have been reported (20–25). Recent work suggests that the combined effects of a paucity of regulatory T cells in the neonatal mouse liver, coupled with the presence of primed dendritic cell populations, trigger NK cell− and $CD8^+$ T cell–mediated destruction of virus-infected cholangiocytes in the RRV model (26, 27).

Zebrafish adaptive immunity develops after the larval stages, between 4 and 6 weeks postfertilization, indicating that it does not play a role in toxin-induced BA in fish (28). The innate immune system, however, is active throughout most of embryogenesis and thus could play a role in toxin-mediated injury (29). To examine the response of innate immune cells to biliary injury in biliatresone-treated larvae, we exposed transgenic fish with green fluorescent protein (GFP)–labeled macrophages [*Tg*(*mpeg-1:GFP*)] and neutrophils [*Tg*(*mpx:GFP*)] to the toxin and then localized these cells using immunohistochemistry at progressive time points (30, 31). This showed progressive accumulation of these innate immune cells around the injured extrahepatic ducts and gallbladder in toxin-treated larvae

(Fig. 3), suggesting a potential contributory role for the innate immune system in toxin-induced biliary injury as identified in the RRV BA model (19). Late accumulation of macrophages around injured intrahepatic ducts is also seen in RRV-infected mice (11), where they are thought to attract neutrophils (32). Macrophage depletion also prevented duct obstruction in the RRV model (33). Macrophages have been implicated as playing a role in human BA (11), and a recent study demonstrated increased hepatic expression of the neutrophil chemoattractant interleukin-8 in BA patients (34), thus suggesting a potential role for neutrophils as a mediator of intrahepatic bile duct injury after the initial damage to the extrahepatic system.

We examined the role of macrophages in toxin-induced biliary injury using a well-described inducible cell ablation methodology (35). Bigenic larvae expressing an NfsB-mCherry fusion protein in macrophages [*Tg*(*mpeg-1:Gal4; UAS:NfsB-mCherry*)] were treated continuously with metronidazole (5 μM) from either 48 or 72 hpf to 120 hpf (5 dpf) to induce macrophage apoptotic cell death. After this period of continuous metronidazole treatment, larvae were exposed to the same metronidazole dose for 2 hours per day. During this period (either 5 to 7 dpf or 5 to 8 dpf), they received continuous biliatresone (either 0.25 or 0.5 μg/ml) followed by immunostaining with the 2F11 antibody and confocal microscopy to evaluate extrahepatic biliarymorphology. Macrophage ablation was monitored in live larvae and showed reduction of mCherry-positive macrophages after exposure to metronidazole. Of 27 larvae imaged for these experiments, 20 larvae had no detectable mCherry-positive cells, and 7 larvae had a small number (<4) of mCherry-positive cells in the intestine. All of these larvae were highly sensitive to biliatresone (fig. S6). These experiments show that macrophages are recruited to bile ducts injured by biliatresone, but that they are not required for biliatresone toxicity.

Bile flow requirement for biliatresone toxicity

We hypothesized that the selective biliary toxicity of biliatresone or one of its metabolites resulted from its secretion and concentration in bile. To test this hypothesis, we examined the effect of the toxin in larvae that lacked intrahepatic bile ducts, predicting that biliatresone would be inactive in these larvae because bile flow to the extrahepatic system was disrupted. We first examined biliatresone-treated wild-type larvae that had been treated with the γ-secretase inhibitor *N*-[(3,5--difluorophenyl)acetyl]-L-alanyl-2-phenyl]glycine-1,1-dimethylethyl ester (DAPT), an inhibitor of Notch signaling that blocks intrahepatic bile duct development (36). Although the gallbladder is small in DAPT-treated larvae (presumably because of the absence of bile flow), we reasoned that the morphology would be preserved after exposure to biliatresone, again because of the absence or marked reduction of bile flow. Consistent with this prediction, gallbladder morphology was indistinguishable in the DAPT-treated controls and toxin-treated larvae that were also treated with DAPT (fig. S9 and table S1).

We next examined the effect of biliatresone in larvae that lack intrahepatic bile ducts because of a genetic mutation. The mutant examined, *ductbend*, was identified in an independent chemical mutagenesis screen formutations that disrupt biliary development. *ductbend* exhibits a pattern of Mendelian recessive inheritance over five generations and is

lethal by 10 to 12 dpf. Confocal microscopy of *ductbend* larvae immunostained with the 2F11 antibody showed few, if any, intrahepatic ducts, but a small gallbladder and patent extrahepatic ducts (Fig. 4). Other phenotypic defects include delayed branchial arch development and intestinal and liver hypoplasia (fig. S10), thus indicating that the affected gene plays multiple developmental roles. Biliatresone was predicted to be inactive in homozygous *ductbend* larvae because bile flow to the extrahepatic system is severely reduced (as in DAPT-treated wild-type larvae). Unexpectedly, gallbladder and extrahepatic duct morphology was disrupted in the toxin-treated mutant larvae compared with untreated mutant larvae, and the degree of injury in many appeared greater than in toxin-treated wild-type larvae (Fig. 4, A and B versus C and D, and fig. S11).

Together, the data from DAPT-treated and *ductbend* larvae argue that the selective biliary toxicity of biliatresone arises as a result of its secretion and concentration in bile, but that genetic modifiers can override this by sensitizing extrahepatic duct and gallbladder epithelial cells to very low levels of the toxin present in either bile or extracellular fluid. In *ductbend*, biliatresone could conceivably enter extracellular fluid either from the vasculature or directly from the aqueous medium in which mutant larvae are reared.

Conserved synteny between *ductbend* and human BA susceptibility loci

To gain insight into the mechanism underlying the sensitization of *ductbend* mutants to biliatresone, we carried out whole-exome sequencing of mutant larvae and their wild-type siblings (n = 100 larvae in each pool). In the mutant pool, we identified a region of homozygosity located on chromosome 22 (nucleotides 27,387,718 to 27,758,148) that was confirmed with genetic mapping (discussed below). Analyses of gene synteny in this region showed that it was homologous to a region of human chromosome 10 (10q25.1; formerly 10q24.2) that was identified as a BA susceptibility locus in a GWAS of Han Chinese patients (Fig. 4E) (3). This association was confirmed in three independent studies of Chinese, Thai, and Caucasian BA patients (37–39). Neither coding sequence mutations nor consistent changes in expression levels have been found in BA patients for the two genes adjacent to the 10q25.1 markers (*XPNPEP-1*, a prolyl aminopeptidase, and *ADD3*, which encodes γ-adducin, a cytoskeletal F-actin capping protein). Expression of *add3* and *xpnpep-1* orthologs was comparable in *ductbend* mutant and wild-type larvae (fig. S12). Coding sequence mutations were not seen in either gene in the exome sequencing.

The critical region surrounding the *ductbend* locus on zebrafish chromosome 22 also has conserved synteny with genes that map to human chromosome 16 (16p13.3; Fig. 4E). A singleton SNP (single-nucleotide polymorphism) within this region (rs17139085), subsequently shown to be adjacent to the *RBFOX1* gene, had the most significant disease association in the human BA-GWAS study (3). No further analysis of this SNP was performed in this or subsequent studies. The zebrafish *RBFOX1* ortholog does not map to chromosome 22, but the orthologs of several adjacent genes do. Three of these genes that are in close proximity to each other (<0.3 Mb) had missense coding sequence mutations in *ductbend*: *slx4*, a scaffold protein that plays a role in DNA maintenance and repair (40); *glis2*, a zinc finger transcription factor that is mutated in patients with recessive nephronophthisis, a heritable cause of kidney failure (41); and *adcy9*, an adenylate cyclase

(42). None of the mutations were predicted to alter gene function, and genetic mapping experiments placed *slx4* ~1 cM (>0.6 Mb) from the *ductbend* locus (six recombinants at SNP 27434434 in 658 meioses; Fig. 4E), thus arguing that neither it, *glis2*, nor *adcy9* is the responsible gene.

Although our current data are not sufficient to molecularly characterize the *ductbend* gene, its proximity to human BA susceptibility loci orthologs (10q25.1 and 16p13.3 genomic regions) does support the idea that a common mechanism underlies susceptibility to biliary injury in the *Dysphania* BA syndrome and human BA. The pleiotropic developmental defects present in homozygous *ductbend* mutants argue that in humans, BA susceptibility would likely be imparted by hypomorphic rather than null alleles of the *ductbend* homolog.

Effect of biliatresone on mammalian cholangiocytes

We previously demonstrated that extrahepatic cholangiocyte primary cilia are decreased in both human BA and the mouse RRV BA model (43, 44). For this reason, we examined cilia in primary neonatal mouse extrahepatic cholangiocytes treated with either biliatresone or the nontoxic isoflavanone-3 that copurifies with biliatresone. Cells treated with biliatresone, but not with isoflavanone-3, had a reduction in primary cilia as determined by staining with antibodies against acetylated α-tubulin (fig. S13, A to C and J). Immunostaining of these cells for cellular tubulin demonstrated a dose-dependent decrease in visible microtubules (figs. S13, D to F, and S14), suggesting that biliatresone, but not isoflavanone-3, decreased microtubule stability. Mouse hepatocytes lack primary cilia; however, primary cultures of neonatal mouse hepatocytes treated with biliatresone showed minimal changes in cellular tubulin staining when treated with biliatresone at 3 μg/ml (fig. S13, G to I) and only mild disruption of cellular tubulin when treated with the highest dose of biliatresone (5 μg/ml; fig. S15, A and B). Primary adult hepatocytes also showed only mild changes in organization of cellular tubulin after treatment with biliatresone even at doses as high as 5 μg/ml (fig. S15, C and D).

Human BA and the BA-like syndrome seen in *Sox17* haploinsufficient mice are both characterized by loss of integrity of the epithelial monolayer lining the extrahepatic ducts (45). Disruption of the gall-bladder epithelium is also an early finding in zebrafish larvae exposed to biliatresone (Figs. 1 and 2 and fig. S4). We therefore examined the effect of biliatresone on epithelial integrity in a three-dimensional mammalian cell culture system in which cholangiocytes polarize and form spheroid monolayers with distinct lumens. Treatment with isoflavanone-3 had no effect (fig. S16), but treatment with biliatresone caused loss of epithelial monolayer integrity with lumen closure and disruption of apical-basal polarity, as shown by staining for F-actin and the β_1 integrin subunit (Fig. 5A). Although closed spheroids were observed even in untreated or vehicle-treated cells, there was a dose-dependent increase in partial and complete lumen closure, with loss of the monolayer, after biliatresone treatment (Fig. 5B). In contrast, treatment with betavulgarin, which had no effect on zebrafish larvae, did not disrupt polarity or result in loss of the monolayer or lumen closure in cholangiocyte spheroids, but cells were consistently more columnar and spheroid lumens were smaller than for vehicle-treated cells (Fig. 5A and fig. S17).

DISCUSSION

The etiology of BA is unknown, although there is evidence implicating an environmental exposure—either infectious or toxic—in genetically susceptible individuals. We report here the activities of the naturally occurring isochalcone, biliatresone, which we have isolated and identified; it is the first toxin known to cause selective destruction of the extrahepatic biliary tree. Zebrafish larvae exposed to biliatresone develop a pattern of extrahepatic biliary damage that strongly resembles the pathology observed in BA in humans. These findings suggest that exposure to structurally related compounds in food or from other environmental sources could be an important triggering event in human BA.

The chemical structure of biliatresone has not been previously reported, and biliatresone is the only structurally characterized plant isochalcone with an exomethylene ketonemoiety. Although the synthetic pathway used by *Dysphania* plants to produce biliatresone is not known, structural analyses suggest that biliatresone might result from the ring opening of one of the copurifying compounds, either betavulgarin or the previously uncharacterized isoflavanone-3. Alternatively, biliatresone may serve as a precursor to the other compounds we isolated. A *Clostridium* species found in the human intestinal microbiota cleaves isoflavonoids found in widely consumed soy products to produce a metabolite with the same exomethylene ketone structure as biliatresone (46–48). This raises the intriguing possibility that human intestinal bacteria could produce toxins resembling biliatresone through modification of nontoxic precursors, such as betavulgarin, which is found in common foods, including sugar beet, table beet, and chard (16, 17). It is conceivable that biliatresone itself or a structurally related toxic compound is found in plants that are normally consumed by humans.

The zebrafish and mammalian cell data presented here suggest that biliatresone can alter the integrity of the cholangiocyte monolayer in the gallbladder and extrahepatic ducts. Over time in vivo, this could result in duct obstruction, which is a defining feature of human BA and is consistently observed in animal models of the disease, including the mouse RRV and *Sox17* haploinsufficiency models and epidemic BA in livestock (45, 49, 50). Although we have not defined a mechanism to account for the effect of biliatresone on cholangiocyte monolayer integrity, the spheroid data demonstrate that biliatresone disrupts apical-basolateral polarity. On the basis of our cell culture experiments that demonstrate a biliatresone-induced destabilization of cellular tubulin, we speculate that this could occur through an effect on microtubules, which play an important role in lumen formation and maintenance of polarity in several types of epithelial cells, including cholangiocytes (51, 52).

The effect of biliatresone on cholangiocyte primary cilia also suggests that disruption of planar cell polarity (PCP) proteins may be part of the toxin’s mechanism of action on cholangiocytes. PCP signaling is required for the assembly and maintenance of primary and motile cilia (53, 54) and has been shown to play an important role in apical-basal polarity, in part through an effect on microtubules (55). PCP signaling has been linked to biliary defects in developing zebrafish (56). Although extrahepatic bile duct cilia are decreased in human BA and the mouse RRV model of BA (44), neither toxin-treated zebrafish nor *Sox17*

haploinsufficient mice demonstrated obvious abnormalities in ductal cilia; however, this may reflect redundancy of vertebrate polarity pathways. Regardless, our data support an effect of biliatresone on cholangiocyte polarity and monolayer integrity and suggest that understanding how the toxin disrupts these may yield important mechanistic insights into human BA.

The zebrafish model of biliary injury we describe here will also aid in understanding both the pathogenesis and clinical course of human BA. The zebrafish is a powerful platform for genetic and chemical modifier screens and has the potential to generate clinically relevant insights into the toxin's mechanism of action. As an example, our experiments showing inactivity of biliatresone in DAPT-treated larvae argue that its selectivity for cholangiocytes is in part related to its secretion into bile. Persistent activity of biliatresone in larvae in which macrophages were ablated suggests that these innate immune cells do not play an important role in the *Dysphania* BA model, unlike the RRV model. Neutrophil-mediated injury could contribute to biliatresone-mediated biliary toxicity, and this will need to be tested when transgenic lines for ablation of this cell type are available.

Our discovery of *ductbend*, its sensitization to biliatresone, and its genetic mapping to a conserved BA susceptibility locus argue that the molecular characterization of this mutant will generate insight into genetic factors influencing BA. Indeed, although it is conceivable that the proximity of the *ductbend* gene to the zebrafish 10q25.1 and 16p13.3 orthologs occurred by chance, this is statistically highly unlikely, and we believe that this is more likely to be the result of its position within a large, ancestral gene cluster. Coexpression of genes within such clusters is, in many instances, thought to arise from positive selection rather than leaky expression (57, 58). On this basis, we speculate that a subset of the genes within the *ductbend* cluster is required for biliary homeostasis. It is thus conceivable that variants of several genes within this cluster, and not just the *ductbend* homolog, could alter BA susceptibility in humans.

Syntenic relationships within large gene clusters often change during evolution (58, 59), and the cluster spanning the *ductbend* locus was disrupted during the amphibian-to-reptile evolutionary transition (www.ensembl.org). Should there be co-regulated expression of the genes within the 10q25.1 and 16p13.3 human BA susceptibility loci, this must occur in trans. Although this most likely involves the action of a shared transcription factor, it is conceivable that a single regulatory element (an enhancer) modulates the expression of genes that are now positioned on different chromosomes (60–62). Molecular characterization of *ductbend* will help us address questions related to the organization and interaction of these and other BA susceptibility loci.

In summary, we have shown that a previously uncharacterized plant isochalcone, biliatresone, exerts a specific, localized destructive effect on the extrahepatic biliary system in a zebrafish model. These data, combined with data showing disruption of cellular polarity and lumen integrity in a mouse cholangiocyte spheroid model, lead us to conclude that biliatresone is highly likely to be the toxic cause of the BA syndrome in the Australian livestock. Whether exposure to biliatresone or a related environmental agent can be directly linked to human BA is unknown, and understanding its relevance to this human disease will

require further study. A detailed study of all of the manifestations of BA, including the intrahepatic biliary injury that uniformly occurs after the initial extrahepatic injury in BA, will require additional animal models: a chronic injury model in the zebrafish system and a rodent model, which will require access to increased quantities of biliatresone. Nonetheless, the in vitro and in vivo injury models we have developed should prove useful in understanding both the mechanism of the inciting event in BA and biliary injury in general, and in identifying similar toxic compounds to which humans are exposed.

MATERIALS AND METHODS

Study design

This study was designed to test the effect of *Dysphania* plant extracts using a screen for biliary secretion in live zebrafish larvae. The in vivo screen is a surrogate for patency of the extrahepatic biliary system and biliary anatomy. The effects of the toxin were confirmed with morphological studies of the biliary system. All experiments were performed a minimum of six times with a minimum of 50 individual larvae. The duration of the treatments (endpoints) was chosen empirically on the basis of the effect of the toxin in the screening assay. The screening and confirmatory assays were performed by four investigators. Confirmatory assays performed in zebrafish and cultured cells were evaluated by blinded investigators.

Plant material

A mixed sample of *D. glomulifera* ssp. *glomulifera* (Nees) Paul G. Wilson and *D. Littoralis* R. Br. (Chenopodiaceae) (~2.8 kg) was collected from the exposed flats of the Burrinjuck Dam, along the Hume Weir, near Albury, New South Wales, Australia (latitude −36.003°, longitude 147.139°) in March 2008. The plants in the collection were identified at the Royal Botanic Gardens, Melbourne, Australia; vouchers for the population are housed at the National Herbarium of Victoria (Melbourne, Australia). The plants were frozen until shipment (−18°C) and shipped on dry ice to the authors' laboratories in April 2009 under a plant import permit from Animal Plant Health and Inspection Service, U.S. Department of Agriculture (permit no. P37-08-00668, 21 May 2008). Individual plants were removed from the frozen material, and voucher specimens were deposited in the herbarium of the University of the Sciences in Philadelphia. The plants were kept frozen at −80°C until analysis. A brief scheme describing plant extraction and fractionation, with purification of biliatresone, is described in fig. S2.

Zebrafish bioassay and analyses

Zebrafish embryos and larvae reared in 24- and 96-well plates were exposed to lyophilized plant extracts resuspended in anhydrous DMSO for 24 to 72 hours (final concentration, 1% DMSO in embryo medium). The concentrations of extracts varied with the subfraction. For the original subfractions, concentrations of 5 to 50 μg/ml were tested. The final subfractions were tested at 0.0625 to 1.0 μg/ml. Embryo medium with extract was exchanged daily. After treatment, larvae were soaked in either PED-6 phospholipid (Invitrogen), the long-chain fatty acid Bodipy-C16 (Invitrogen), or the short-chain fatty acid Bodipy-C5 (Invitrogen) for 4 hours as previously described (63). Gallbladder and intestinal fluorescence in the treated

and control larvae were examined with a stereomicroscope (Olympus MVX-10).Quantification of fluorescence was performed with ImageJ software to calculate corrected total fluorescence over the region of the gallbladder (CTCF in ImageJ). Larvae were processed for histology, immunostaining, and confocal microscopy as previously described (36). All assays were performed in triplicate with at least 25 to 50 treated larvae and an equal number of control larvae. Control experiments to assess the effect on swallowing behavior were performed for each subfraction and for experiments using purified biliatresone as described (64). Larvae were incubated in 50 μM DAPT or *N*-[*N*-(3,5--difluorophenacetyl)-L-alanyl]-*S*-phenylglycine *t*-butyl ester (Sigma-Aldrich) (stock solution of 100 mM in DMSO) as previously described (36).

After treatments, larvae were fixed in 4% paraformaldehyde and immunostained with mouse monoclonal antibody 2F11 (gift from J. Lewis) (65, 66) or processed for histology as previously described (36, 67).

ductbend mutants were recovered in an *N*-ethyl-*N*-nitrosourea mutagenesis screen for mutations that disrupt the metabolismor biliary secretion of fluorescent lipids [as described in (15)]. *ductbend* larvae at 5 dpf have pleiotropic defects, most notably delayed branchial arch development and digestive organ hypoplasia. The mutant larvae lack intrahepatic bile ducts, and their gallbladder and extrahepatic ducts are patent but smaller than in wild-type siblings. The mutation is recessive lethal by 10 to 12 dpf.

Exome sequencing of *ductbend* mutants

Genomic DNA was extracted from pools of 100 5-dpf *ductbend* and sibling larvae with TRIzol (Sigma-Aldrich) and processed for whole-exome sequencing as described (68). Mutation mapping was performed using the MMAPPR protocol (69).

Genetic mapping of the *ductbend* locus

A mapping cross was generated by crossing adult fish heterozygous for the *ductbend* mutation with wild-type fish with the Wik background. F2 mutant *ductbend* larvae ($n = 329$) were examined at 5 dpf for the presence of an SNP within the *slx4* coding region that was identified by exome sequencing (A to G conversion at nucleotide 27434434). SNP mapping of individual mutant larvae was performed via PCR with allele-specific primers generated with dCAPS Finder 2.0 (http://helix.wustl.edu/dcaps/dcaps.html). The forward and reverse primers to amplify the wild-type slx4 allele were ttgccatagtaacagtcgaggcgtggcc and agtgtgtgtgaagccttgtaatgttgtt. Hpa II digest of the wild-type PCR product generated 148-, 87-, and 26-bp (base pair) fragments, whereas the mutant fragment gave 148- and 113-bp fragments.

Mammalian cells

The small cholangiocyte cell line used for spheroid culture was as described (70). Neonatal extrahepatic cholangiocytes were isolated by outgrowth from 0- to 3-day-old BALB/c mouse pups. Briefly, ducts were dissected away from stroma and surrounding cells and then embedded and cultured in a thick collagen gel (2 mg/ml) for 3 to 4 weeks. Cells were split and cultured on thin collagen–coated (1 mg/ml) dishes for an additional 2 weeks before use

(71). Mouse neonatal and adult hepatocytes were isolated as described; cells were cultured for 48 hours after isolation before being treated with toxin (72). Cells from an entire litter of pups (at least 10) were used for each individual experiment with neonatal hepatocytes or cholangiocytes.

Toxin treatment and immunostaining

Cells were treated with vehicle (DMSO), biliatresone, betavulgarin, or isoflavanone-3 at doses ranging from 0.5 to 5 μg/ml for 24 hours. Biliatresone was toxic to cholangiocytes (but not hepatocytes) at doses greater than 2 μg/ml. Cells were fixed and stained with antibodies against acetylated α-tubulin (1:5000; Sigma), as a marker of cilia, and cellular tubulin (1:500; Sigma) and with the nuclear stain DAPI. Immunostaining with antibodies against K19 (1:10, Developmental Studies Hybridoma Bank) for cholangiocytes and HNF4-α (1:1000; Abcam) for hepatocytes confirmed that primary cells were at >95% purity. To determine the percentage of cells with cilia, immunostained cilia visible in a given high-power field were counted by a blinded observer (R.G.W.) and expressed as a percentage of the total number of cells, as determined by DAPI nuclear staining.

Spheroid culture

Cells were plated in a collagen-Matrigel mixture (collagen, 4 mg/ml; Matrigel, 3.7 mg/ml; rat tail collagen I and growth factor–reduced, phenol red–free Matrigel; BD Biosciences) in cell culture inserts (Millicell; Millipore) and incubated for 8 days. Media were changed every 2 to 3 days. On day 7, cells were treated with vehicle (DMSO), biliatresone, or betavulgarin at 2 μg/ml. Twenty-four hours after treatment, the cells were fixed with 4% ethanol and stained for F-actin (1:1000; phalloidin–tetramethylrhodamine B isothiocyanate; Santa Cruz Biotechnology) and with an antibody against the integrin β_1 subunit (1:100; Abcam). For quantification of the effect of biliatresone, spheroids were stained for F-actin, and multiple confocal images were acquired. Lumens in the spheroids were assessed by a blinded observer (O.W.-Z.) as being open, closed (no lumen visible), or partially open or narrowed (small visible lumen). Only spheroids imaged at a level with a clearly visible midsection were counted.

Statistics

Statistical significance was calculated by either the one-tailed Student's *t* test or one-way analysis of variance.

Supplementary Material

Refer to Web version on PubMed Central for supplementary material.

Acknowledgments

We are grateful to M. Muthumani for assistance with zebrafish husbandry, C. Dang for assistance with spheroid studies, M. Perepelyuk for assistance with hepatocyte isolation, and the University of Pennsylvania Department of Cell and Developmental Biology Imaging Core for assistance with microscopy. We thank J. Lewis for the gift of mouse monoclonal antibody 2F11. We acknowledge the late Surrey Jacobs for identification of *Dysphania* species plants.

Funding: This work was supported in part by the NIH/National Institute of Diabetes and Digestive and Kidney Center for Molecular Studies in Digestive and Liver Diseases (P30DK050306) and its core facilities. Funding for J.R.P., R.G.W., and M.P. was from the NIH (R01DK092111) and the Fred and Suzanne Biesecker Pediatric Liver Center at The Children's Hospital of Philadelphia. D.L.S. was supported by the Wellcome Trust (grant number 098051).

REFERENCES AND NOTES

1. Haber BA, Russo P. Biliary atresia. Gastroenterol. Clin. North Am. 2003; 32:891–911. [PubMed: 14562580]
2. Zhou K, Lin N, Xiao Y, Wang Y, Wen J, Zou G-M, Gu X, Cai W. Elevated bile acids in newborns with biliary atresia (BA). PLOS One. 2012; 7:e49270. [PubMed: 23166626]
3. Garcia-Barcelo M-M, Yeung M-Y, Miao X-P, Tang CS-M, Cheng G, So M-T, Ngan ES-W, Lui VC-H, Chen Y, Liu X-L, Hui K-JWS, Li L, Guo W-H, Sun X-B, Tou J-F, Chan K-W, Wu X-Z, Song Y-Q, Chan D, Cheung K, Chung PH-Y, Wong KK-Y, Sham P-C, Cherny SS, Tam PK-H. Genome-wide association study identifies a susceptibility locus for biliary atresia on 10q24.2. Hum. Mol. Genet. 2010; 19:2917–2925. [PubMed: 20460270]
4. Rurarz M, Czubkowski P, Chrzanowska K, Cielecka-Kuszyk J, Marczak A, Kaminska D, Pawłowska J. Biliary atresia in children with aberrations involving chromosome 11q. J Pediatr. Gastroenterol. Nutr. 2014; 58:e26–e29. [PubMed: 23752074]
5. Leyva-Vega M, Gerfen J, Thiel BD, Jurkiewicz D, Rand EB, Pawlowska J, Kaminska D, Russo P, Gai X, Krantz ID, Kamath BM, Hakonarson H, Haber BA, Spinner NB. Genomic alterations in biliary atresia suggest region of potential disease susceptibility in 2q37.3. Am. J. Med. Genet. A. 2010; 152A:886–895. [PubMed: 20358598]
6. Tiao M-M, Liou C-W, Huang L-T, Wang P-W, Lin T-K, Chen J-B, Chou Y-M, Huang Y-H, Lin H-Y, Chen C-L, Chuang J-H. Associations of mitochondrial haplogroups B4 and E with biliary atresia and differential susceptibility to hydrophobic bile acid. PLOS Genet. 2013; 9:e1003696. [PubMed: 23966875]
7. Bezerra JA. Potential etiologies of biliary atresia. Pediatr. Transplant. 2005; 9:646–651. [PubMed: 16176425]
8. Riepenhoff-Talty M, Schaekel K, Clark HF, Mueller W, Uhnoo I, Rossi T, Fisher J, Ogra PL. Group A rotaviruses produce extrahepatic biliary obstruction in orally inoculated newborn mice. Pediatr. Res. 1993; 33:394–399. [PubMed: 8386833]
9. Tiao M-M, Tsai S-S, Kuo H-W, Chen C-L, Yang C-Y. Epidemiological features of biliary atresia in Taiwan, a national study 1996–2003. J Gastroenterol. Hepatol. 2008; 23:62–66. [PubMed: 17725591]
10. Rauschenfels S, Krassmann M, Al-Masri AN, Verhagen W, Leonhardt J, Kuebler JF, Petersen C. Incidence of hepatotropic viruses in biliary atresia. Eur. J. Pediatr. 2009; 168:469–476. [PubMed: 18560888]
11. Mack CL, Feldman AG, Sokol RJ. Clues to the etiology of bile duct injury in biliary atresia. Semin. Liver Dis. 2012; 32:307–316. [PubMed: 23397531]
12. Saito T, Shinozaki K, Matsunaga T, Ogawa T, Etoh T, Muramatsu T, Kawamura K, Yoshida H, Ohnuma N, Shirasawa H. Lack of evidence for reovirus infection in tissues from patients with biliary atresia and congenital dilatation of the bile duct. J Hepatol. 2004; 40:203–211. [PubMed: 14739089]
13. Harper P, Plant JW, Unger DB. Congenital biliary atresia and jaundice in lambs and calves. Aust. Vet. J. 1990; 67:18–22. [PubMed: 2334368]
14. Robson, S. New South Wales Animal Health Surveillance. Vol. 2. Sydney, New South Wales, Australia: NSW Department of Primary Industries; 2007. Congenital biliary atresia and jaundice in lambs; p. 2-4.
15. Farber SA, Pack M, Ho SY, Johnson ID, Wagner DS, Dosch R, Mullins MC, Hendrickson HS, Hendrickson EK, Halpern ME. Genetic analysis of digestive physiology using fluorescent phospholipid reporters. Science. 2001; 292:1385–1388. [PubMed: 11359013]
16. Elliger CA, Halloin JM. Phenolics induced in *Beta vulgaris* by *Rhizoctonia solani* infection. Phytochemistry. 1994; 37:691–693. [PubMed: 7765684]

17. Geigert J, Stermitz FR, Johnson G, Maag DD. Two phytoalexins from sugarbeet (*Beta vulgaris*) leaves. Tetrahedron. 1973; 29:2703–2706.
18. Lorent K, Yeo S-Y, Oda T, Chandrasekharappa S, Chitnis A, Matthews RP, Pack M. Inhibition of Jagged-mediated Notch signaling disrupts zebrafish biliary development and generates multi-organ defects compatible with an Alagille syndrome phenocopy. Development. 2004; 131:5753–5766. [PubMed: 15509774]
19. Feldman AG, Mack CL. Biliary atresia: Cellular dynamics and immune dysregulation. Semin. Pediatr. Surg. 2012; 21:192–200. [PubMed: 22800972]
20. Bessho K, Bezerra JA. Biliary atresia: Will blocking inflammation tame the disease? Annu. Rev. Med. 2011; 62:171–185. [PubMed: 21226614]
21. Shivakumar P, Sabla G, Mohanty S, McNeal M, Ward R, Stringer K, Caldwell C, Chougnet C, Bezerra JA. Effector role of neonatal hepatic $CD8^+$ lymphocytes in epithelial injury and autoimmunity in experimental biliary atresia. Gastroenterology. 2007; 133:268–277. [PubMed: 17631148]
22. Shivakumar P, Sabla GE, Whitington P, Chougnet CA, Bezerra JA. Neonatal NK cells target the mouse duct epithelium via Nkg2d and drive tissue-specific injury in experimental biliary atresia. J Clin. Invest. 2009; 119:2281–2290. [PubMed: 19662681]
23. Feldman AG, Tucker RM, Fenner EK, Pelanda R, Mack CL. B cell deficient mice are protected from biliary obstruction in the rotavirus-induced mouse model of biliary atresia. PLOS One. 2013; 8:e73644. [PubMed: 23991203]
24. Lages CS, Simmons J, Chougnet CA, Miethke AG. Regulatory T cells control the CD8 adaptive immune response at the time of ductal obstruction in experimental biliary atresia. Hepatology. 2012; 56:219–227. [PubMed: 22334397]
25. Tucker RM, Feldman AG, Fenner EK, Mack CL. Regulatory T cells inhibit Th1 cell-mediated bile duct injury in murine biliary atresia. J Hepatol. 2013; 59:790–796. [PubMed: 23685050]
26. Qiu Y, Yang J, Wang W, Zhao W, Peng F, Xiang Y, Chen G, Chen T, Chai C, Zheng S, Watkins DJ, Feng J. HMGB1-promoted and TLR2/4-dependent NK cell maturation and activation take part in rotavirus-induced murine biliary atresia. PLOS Pathog. 2014; 10:e1004011. [PubMed: 24651485]
27. Saxena V, Shivakumar P, Sabla G, Mourya R, Chougnet C, Bezerra JA. Dendritic cells regulate natural killer cell activation and epithelial injury in experimental biliary atresia. Sci. Transl. Med. 2011; 3:102ra94.
28. Lam SH, Chua HL, Gong Z, Lam TJ, Sin YM. Development and maturation of the immune system in zebrafish, *Danio rerio*: A gene expression profiling, in situ hybridization and immunological study. Dev. Comp. Immunol. 2004; 28:9–28. [PubMed: 12962979]
29. Novoa B, Figueras A. Zebrafish: Model for the study of inflammation and the innate immune response to infectious diseases. Adv. Exp. Med. Biol. 2012; 946:253–275. [PubMed: 21948373]
30. Ellett F, Pase L, Hayman JW, Andrianopoulos A, Lieschke GJ. *mpeg1* promoter transgenes direct macrophage-lineage expression in zebrafish. Blood. 2011; 117:e49–e56. [PubMed: 21084707]
31. Renshaw SA, Loynes CA, Trushell DMI, Elworthy S, Ingham PW, Whyte MKB. A transgenic zebrafish model of neutrophilic inflammation. Blood. 2006; 108:3976–3978. [PubMed: 16926288]
32. Mohanty SK, Ivantes CAP, Mourya R, Pacheco C, Bezerra JA. Macrophages are targeted by rotavirus in experimental biliary atresia and induce neutrophil chemotaxis by Mip2/Cxcl2. Pediatr. Res. 2010; 67:345–351. [PubMed: 20234283]
33. Li J, Bessho K, Shivakumar P, Mourya R, Mohanty SK, Dos Santos JL, Miura IK, Porta G, Bezerra JA. Th2 signals induce epithelial injury in mice and are compatible with the biliary atresia phenotype. J Clin. Invest. 2011; 121:4244–4256. [PubMed: 22005305]
34. Bessho K, Mourya R, Shivakumar P, Walters S, Magee JC, Rao M, Jegga AG, Bezerra JA. Gene expression signature for biliary atresia and a role for interleukin-8 in pathogenesis of experimental disease. Hepatology. 2014; 60:211–223. [PubMed: 24493287]
35. White DT, Mumm JS. The nitroreductase system of inducible targeted ablation facilitates cell-specific regenerative studies in zebrafish. Methods. 2013; 62:232–240. [PubMed: 23542552]
36. Lorent K, Moore JC, Siekmann AF, Lawson N, Pack M. Reiterative use of the notch signal during zebrafish intrahepatic biliary development. Dev. Dyn. 2010; 239:855–864. [PubMed: 20108354]

37. Kaewkiattiyot S, Honsawek S, Vejchapipat P, Chongsrisawat V, Poovorawan Y. Association of X-prolyl aminopeptidase 1 rs17095355 polymorphism with biliary atresia in Thai children. Hepatol. Res. 2011; 41:1249–1252. [PubMed: 22118303]
38. Tsai EA, Grochowski CM, Loomes KM, Bessho K, Hakonarson H, Bezerra JA, Russo PA, Haber BA, Spinner NB, Devoto M. Replication of a GWAS signal in a Caucasian population implicates *ADD3* in susceptibility to biliary atresia. Hum. Genet. 2014; 133:235–243. [PubMed: 24104524]
39. Cheng G, Tang CS-M, Wong EH-M, Cheng WW-C, So M-T, Miao X, Zhang R, Cui L, Liu X, Ngan ES-W, Lui VC-H, Chung PH-Y, Chan IH-Y, Liu J, Zhong W, Xia H, Yu J, Qiu X, Wu X-Z, Wang B, Dong X, Tou J, Huang L, Yi B, Ren H, Chan EK-W, Ye K, O'Reilly PF, Wong KK-Y, Sham P-C, Cherny SS, Tam PK-H, Garcia-Barcelo M-M. Common genetic variants regulating *ADD3* gene expression alter biliary atresia risk. J Hepatol. 2013; 59:1285–1291. [PubMed: 23872602]
40. Kim Y, Spitz GS, Veturi U, Lach FP, Auerbach AD, Smogorzewska A. Regulation of multiple DNA repair pathways by the Fanconi anemia protein SLX4. Blood. 2013; 121:54–63. [PubMed: 23093618]
41. Attanasio M, Uhlenhaut NH, Sousa VH, O'Toole JF, Otto E, Anlag K, Klugmann C, Treier A-C, Helou J, Sayer JA, Seelow D, Nürnberg G, Becker C, Chudley AE, Nürnberg P, Hildebrandt F, Treier M. Loss of GLIS2 causes nephronophthisis in humans and mice by increased apoptosis and fibrosis. Nat. Genet. 2007; 39:1018–1024. [PubMed: 17618285]
42. Hacker BM, Tomlinson JE, Wayman GA, Sultana R, Chan G, Villacres E, Disteche C, Storm DR. Cloning, chromosomal mapping, and regulatory properties of the human type 9 adenylyl cyclase (ADCY9). Genomics. 1998; 50:97–104. [PubMed: 9628827]
43. Chu AS, Russo PA, Wells RG. Cholangiocyte cilia are abnormal in syndromic and nonsyndromic biliary atresia. Mod. Pathol. 2012; 25:751–757. [PubMed: 22301700]
44. Karjoo S, Hand NJ, Loarca L, Russo PA, Friedman JR, Wells RG. Extrahepatic cholangiocyte cilia are abnormal in biliary atresia. J Pediatr. Gastroenterol. Nutr. 2013; 57:96–101. [PubMed: 23609896]
45. Uemura M, Ozawa A, Nagata T, Kurasawa K, Tsunekawa N, Nobuhisa I, Taga T, Hara K, Kudo A, Kawakami H, Saijoh Y, Kurohmaru M, Kanai-Azuma M, Kanai Y. *Sox17* haploin-sufficiency results in perinatal biliary atresia and hepatitis in C57BL/6 background mice. Development. 2013; 140:639–648. [PubMed: 23293295]
46. Hur HG, Beger R, Heinze T, Lay J, Freeman J, Dore J, Rafii F. Isolation of an anaerobic intestinal bacterium capable of cleaving the C-ring of the isoflavonoid daidzein. Arch. Microbiol. 2002; 178:8–12. [PubMed: 12070764]
47. Kelly GE, Nelson C, Waring MA, Joannou GE, Reeder AY. Metabolites of dietary (soya) isoflavones in human urine. Clin. Chim. Acta. 1993; 223:9–22. [PubMed: 8143372]
48. Joannou GE, Kelly GE, Reeder AY, Waring M, Nelson C. A urinary profile study of dietary phytoestrogens. The identification and mode of metabolism of new isoflavonoids. J Steroid Biochem. Mol. Biol. 1995; 54:167–184. [PubMed: 7662591]
49. Gibelli NEM, Tannuri U, de Mello ES, Rodrigues CJ. Bile duct ligation in neonatal rats: Is it a valid experimental model for biliary atresia studies? Pediatr. Transplant. 2009; 13:81–87. [PubMed: 18452497]
50. Thomson J. On congenital obliteration of the bile-ducts. Edinb. Med. J. 1892; 37:523–531.
51. Akhtar N, Streuli CH. An integrin-ILK-microtubule network orients cell polarity and lumen formation in glandular epithelium. Nat. Cell Biol. 2013; 15:17–27. [PubMed: 23263281]
52. Tanimizu N, Kikkawa Y, Mitaka T, Miyajima A. α1- and α5-containing laminins regulate the development of bile ducts via β1 integrin signals. J Biol. Chem. 2012; 287:28586–28597. [PubMed: 22761447]
53. Zilber Y, Babayeva S, Seo JH, Liu JJ, Mootin S, Torban E. The PCP effector Fuzzy controls cilial assembly and signaling by recruiting Rab8 and Dishevelled to the primary cilium. Mol. Biol. Cell. 2013; 24:555–565. [PubMed: 23303251]
54. Gray RS, Abitua PB, Wlodarczyk BJ, Szabo-Rogers HL, Blanchard O, Lee I, Weiss GS, Liu KJ, Marcotte EM, Wallingford JB, Finnell RH. The planar cell polarity effector Fuz is essential for

targeted membrane trafficking, ciliogenesis and mouse embryonic development. Nat. Cell Biol. 2009; 11:1225–1232. [PubMed: 19767740]

55. Tao H, Inoue K-I, Kiyonari H, Bassuk AG, Axelrod JD, Sasaki H, Aizawa S, Ueno N. Nuclear localization of Prickle2 is required to establish cell polarity during early mouse embryogenesis. Dev. Biol. 2012; 364:138–148. [PubMed: 22333836]
56. Cui S, Capecci LM, Matthews RP. Disruption of planar cell polarity activity leads to developmental biliary defects. Dev. Biol. 2011; 351:229–241. [PubMed: 21215262]
57. Hurst LD, Pál C, Lercher MJ. The evolutionary dynamics of eukaryotic gene order. Nat. Rev. Genet. 2004; 5:299–310. [PubMed: 15131653]
58. Wang G-Z, Chen W-H, Lercher MJ. Coexpression of linked gene pairs persists long after their separation. Genome Biol. Evol. 2011; 3:565–570. [PubMed: 21737396]
59. Al-Shahrour F, Minguez P, Marqués-Bonet T, Gazave E, Navarro A, Dopazo J. Selection upon genome architecture: Conservation of functional neighborhoods with changing genes. PLOS Comput. Biol. 2010; 6:e1000953. [PubMed: 20949098]
60. Branco MR, Pombo A. Intermingling of chromosome territories in interphase suggests role in translocations and transcription-dependent associations. PLOS Biol. 2006; 4:e138. [PubMed: 16623600]
61. Harmston N, Lenhard B. Chromatin and epigenetic features of long-range gene regulation. Nucleic Acids Res. 2013; 41:7185–7199. [PubMed: 23766291]
62. Bateman JR, Johnson JE, Locke MN. Comparing enhancer action in *cis* and in *trans*. Genetics. 2012; 191:1143–1155. [PubMed: 22649083]
63. Clifton JD, Lucumi E, Myers MC, Napper A, Hama K, Farber SA, Smith AB III, Huryn DM, Diamond SL, Pack M. Identification of novel inhibitors of dietary lipid absorption using zebrafish. PLOS One. 2010; 5:e12386–e12388. [PubMed: 20811635]
64. Abrams J, Davuluri G, Seiler C, Pack M. Smooth muscle caldesmon modulates peristalsis in the wild type and non-innervated zebrafish intestine. Neurogastroenterol. Motil. 2012; 24:288–299. [PubMed: 22316291]
65. Crosnier C, Vargesson N, Gschmeissner S, Ariza-McNaughton L, Morrison A, Lewis J. Delta-Notch signalling controls commitment to a secretory fate in the zebrafish intestine. Development. 2005; 132:1093–1104. [PubMed: 15689380]
66. Zhang D, Golubkov VS, Han W, Correa RG, Zhou Y, Lee S, Strongin AY, Duc P, Dong S. Identification of Annexin A4 as a hepatopancreas factor involved in liver cell survival. Dev. Biol. 2014; 395:96–110. [PubMed: 25176043]
67. Pack M, Solnica-Krezel L, Malicki J, Neuhauss SC, Schier AF, Stemple DL, Driever W, Fishman MC. Mutations affecting development of zebrafish digestive organs. Development. 1996; 123:321–328. [PubMed: 9007252]
68. Kettleborough RNW, Busch-Nentwich EM, Harvey SA, Dooley CM, de Bruijn E, van Eeden F, Sealy I, White RJ, Herd C, Nijman IJ, Fényes F, Mehroke S, Scahill C, Gibbons R, Wali N, Carruthers S, Hall A, Yen J, Cuppen E, Stemple DL. A systematic genome-wide analysis of zebrafish protein-coding gene function. Nature. 2013; 496:494–497. [PubMed: 23594742]
69. Hill JT, Demarest BL, Bisgrove BW, Gorsi B, Su Y-C, Yost HJ. MMAPPR: Mutation mapping analysis pipeline for pooled RNA-seq. Genome Res. 2013; 23:687–697. [PubMed: 23299975]
70. Ueno Y, Alpini G, Yahagi K, Kanno N, Moritoki Y, Fukushima K, Glaser S, LeSage G, Shimosegawa T. Evaluation of differential gene expression by microarray analysis in small and large cholangiocytes isolated from normal mice. Liver Int. 2003; 23:449–459. [PubMed: 14986819]
71. Karjoo S, Wells RG. Isolation of neonatal extrahepatic cholangiocytes. J Vis. Exp. 2014:e51621.
72. Perepelyuk M, Terajima M, Wang AY, Georges PC, Janmey PA, Yamauchi M, Wells RG. Hepatic stellate cells and portal fibroblasts are the major cellular sources of collagens and lysyl oxidases in normal liver and early after injury. Am. J. Physiol. Gastrointest. Liver Physiol. 2013; 304:G605–G614. [PubMed: 23328207]

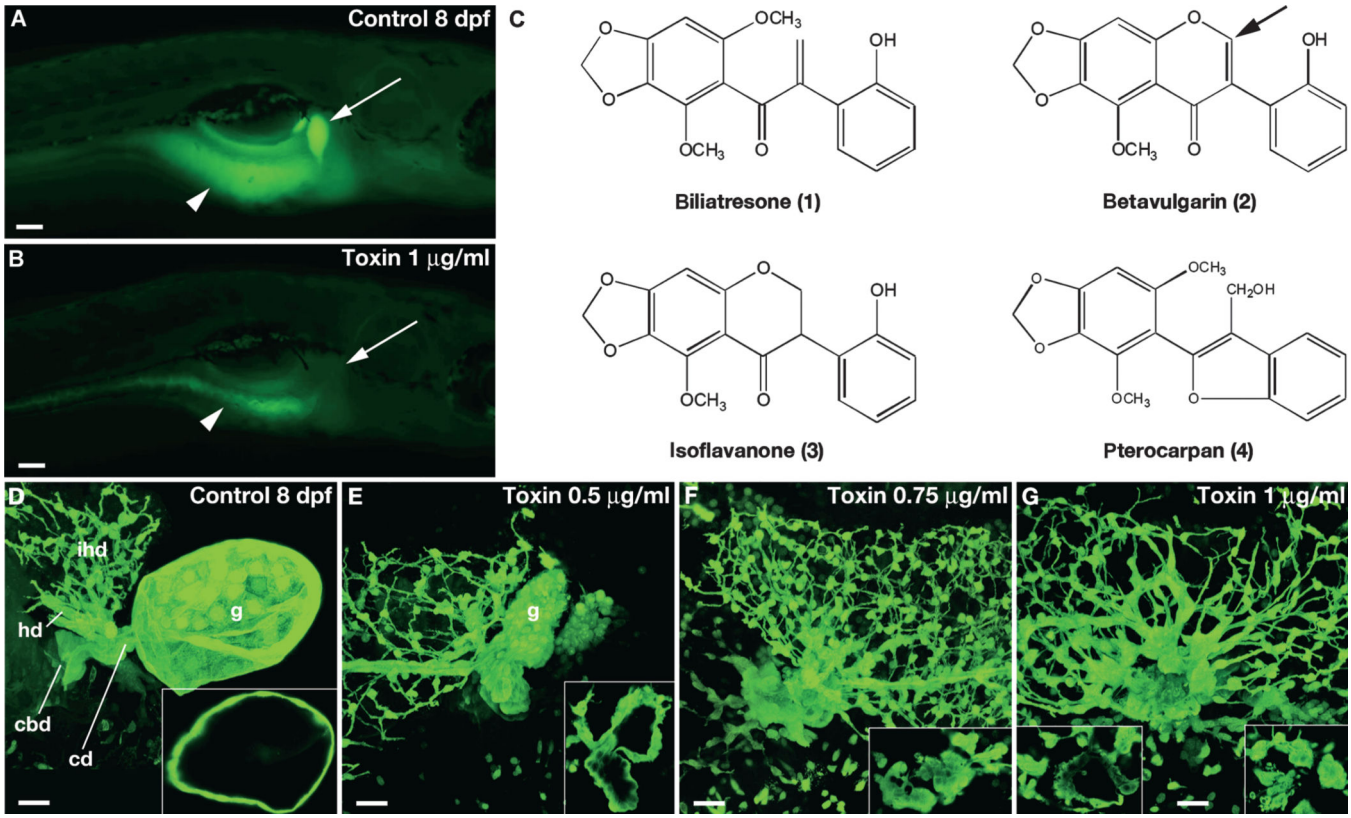

Fig. 1. Biliatresone identification

(**A** and **B**) Lateral fluorescent image of a live 8 dpf wild-type (wt) control larva (A) and a larva treated with biliatresone (B) for 48 hours beginning at 5 dpf (1.0 μg/ml). Both larvae were soaked in Bodipy-C16 for 4 hours before imaging. Gallbladder fluorescence (arrow) is absent, and intestinal fluorescence (arrowheads) is markedly reduced in the toxin-treated larva. (**C**) Chemical structures of biliatresone and related isoflavones noted in the text. Arrow points to site of C-ring cleavage during possible metabolism of betavulgarin to biliatresone. (**D** to **G**) Confocal projections of the gallbladder and extrahepatic bile ducts of 8 dpf immunostained control (D) and toxin-treated (E to G) larvae. Insets show thin (1 μm) confocal sections of gallbladders. Increased doses of the toxin caused progressive changes in morphology of the gallbladder and extrahepatic ducts with preservation of the intrahepatic ducts. The variation seen in intrahepatic duct morphology is within normal limits. g, gallbladder; cd, cystic duct; cbd, common bile duct; ihd, intrahepatic bile ducts; hd, hepatic duct. Scale bars, 100 μm (A and B); 20 μm (D to G).

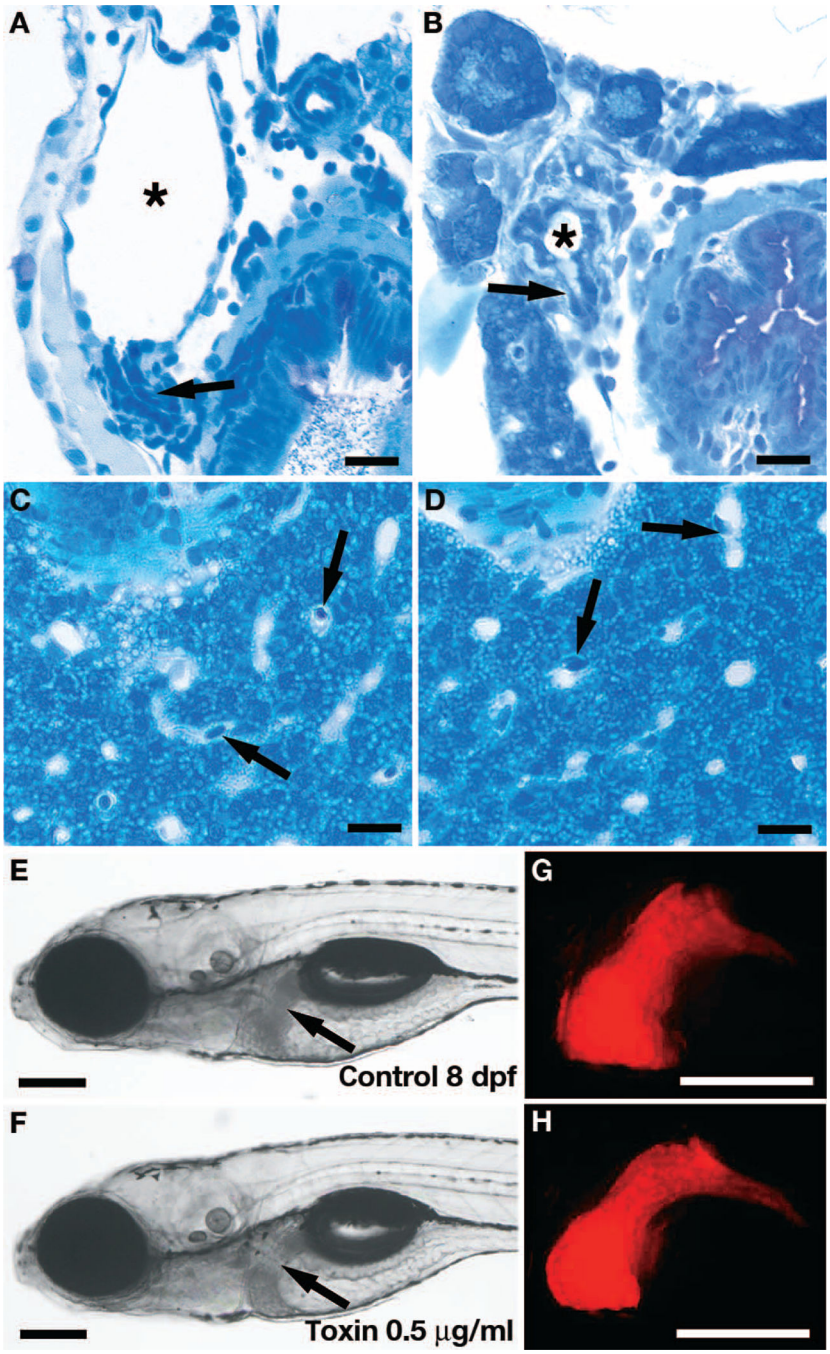

Fig. 2. Biliatresone tissue specificity

(**A** and **B**) Histological cross sections showing severe morphological defects of the gallbladder (asterisks) and cystic duct (arrows) in an 8 dpf biliatresone–treated larva (B) compared with a control larva (A). (**C** and **D**) Normal histological appearance of hepatocytes and liver sinusoids in an 8 dpf toxin-treated larva (D) compared with a control larva (C). Sinusoids (containing nucleated red blood cells; arrows) are the principal vascular channel in the liver of zebrafish larvae; thus, branches of the portal vein and artery are not seen in these histological sections. Intrahepatic bile ducts are too small to be seen. (**E** to **H**)

Bright-field images of live 8 dpf control (E) and toxin-treated (F) *Tg*(*lfabp-RFP*) larvae with corresponding fluorescent images of the liver (G and H). Arrows, liver (E and F). Scale bars, 10 μm (A to D); 200 μm (E to H).

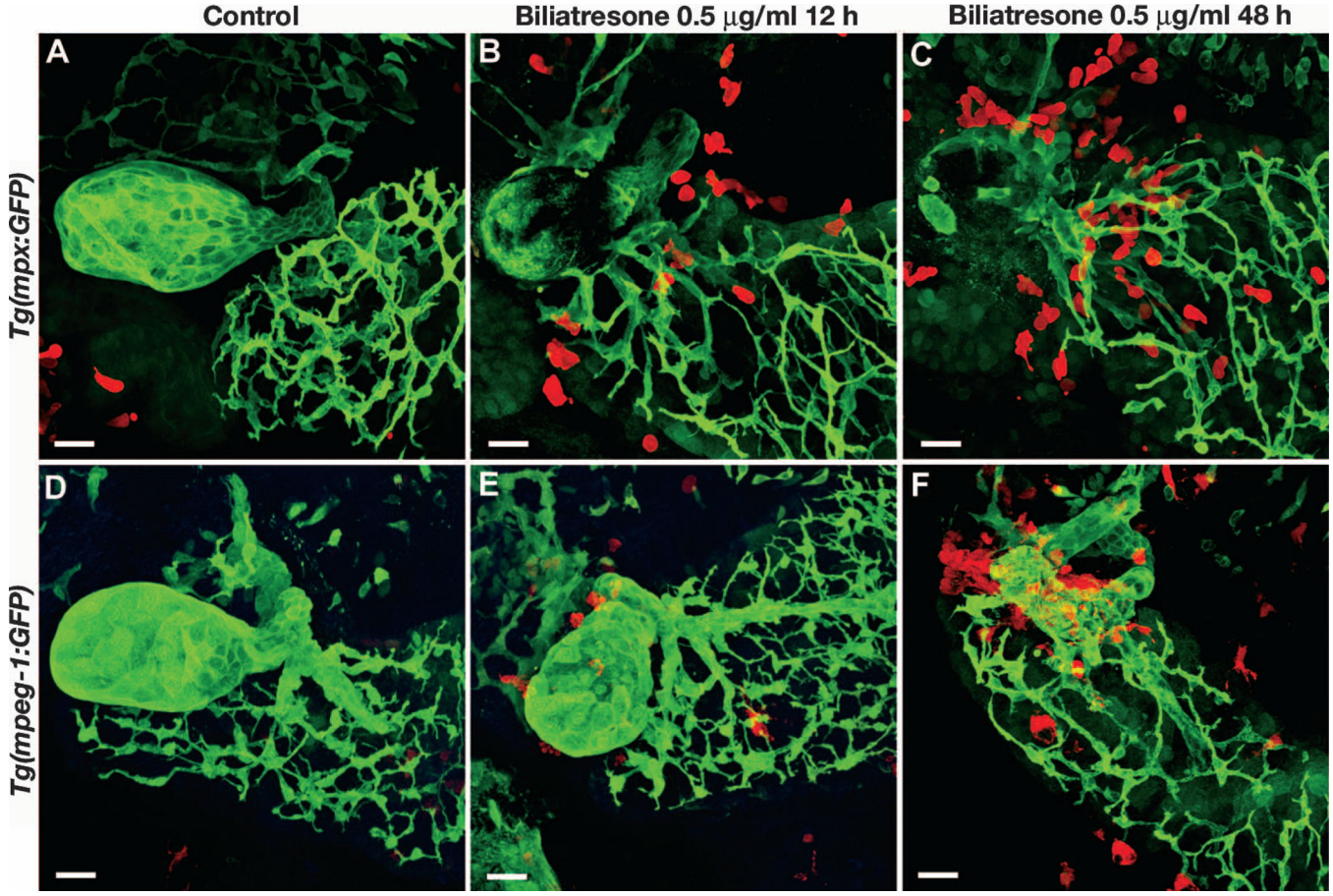

Fig. 3. Innate immune response in biliatresone-treated larvae

Confocal projections through the liver of *Tg*(*mpx:GFP*) and *Tg*(*mpeg-1:GFP*) larvae immunostained with the 2F11 monoclonal antibody (green) and anti-GFP antibody (red). (**A** and **D**) Control larvae (5 dpf) show a well-formed gallbladder. (**B**, **C**, **E**, and **F**) Biliatresone-treated larvae show progressive accumulation of neutrophils (B and C) and macrophages (E and F) with increasing duration of treatment. Twelve-hour biliatresone treatment (B and E) causes milder changes in gallbladder morphology compared with 48-hour treatment (C and F). Biliatresone treatment was initiated at 5 dpf in all larvae. Scale bars, 20 μm.

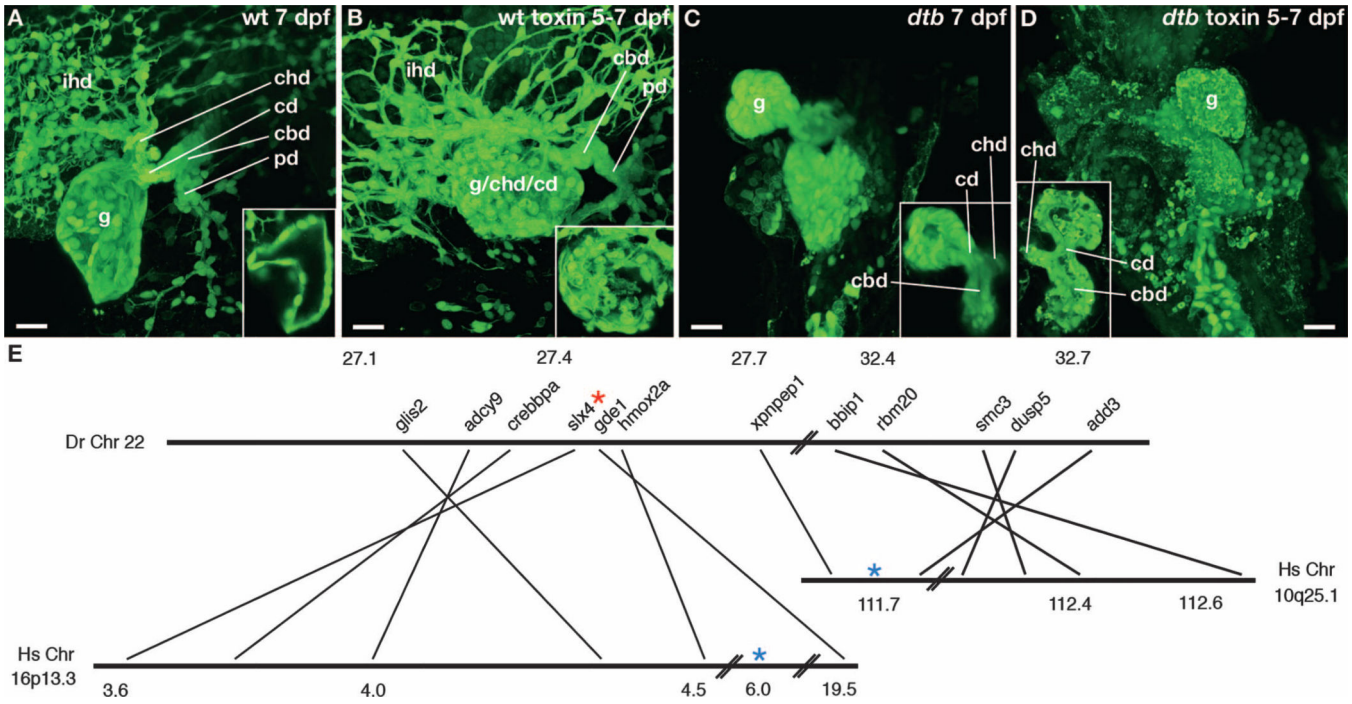

Fig. 4. Zebrafish *ductbend* sensitization

| (**A** to **D**) Confocal projections through the liver and extrahepatic biliary system of control and toxin-treated wt and *ductbend* (*dtb*) larvae. Insets show thin sections through the gallbladder (A and B) or gallbladder and extrahepatic duct (C and D). Compared to the control larvae, extrahepatic BA (A) is evident in the treated wt larva (B), because the three principal components of the extrahepatic system (gallbladder, common bile duct, and cystic duct) distal to the common hepatic duct (chd) cannot be identified. (C) The control *ductbend* larva lacks intrahepatic bile ducts and has a hypoplastic gallbladder. (D) Toxin-induced damage to the extrahepatic system is more pronounced in the treated *ductbend* larva compared with wt (C). wt and *ductbend* larvae were treated with biliatresone (1 μg/ml) from 5 to 7 dpf. (**E**) Simplified genetic synteny map of the *ductbend* locus indicating the position of genes relative to their human orthologs at the BA susceptibility loci (16p13.3 and 10q25.1). Numbers refer to chromosomal location in Mb. Blue asterisks, positions of SNPs in BA susceptibility loci; red asterisk, position of SNP 27434434, ~1 centimorgan (cM) (0.6 Mb) from the *ductbend* locus. ihd, intrahepatic bile ducts; g, gallbladder; cbd, common bile duct; cd, cystic duct; chd, common hepatic duct; pd, pancreatic duct. Scale bars, 20 μm.

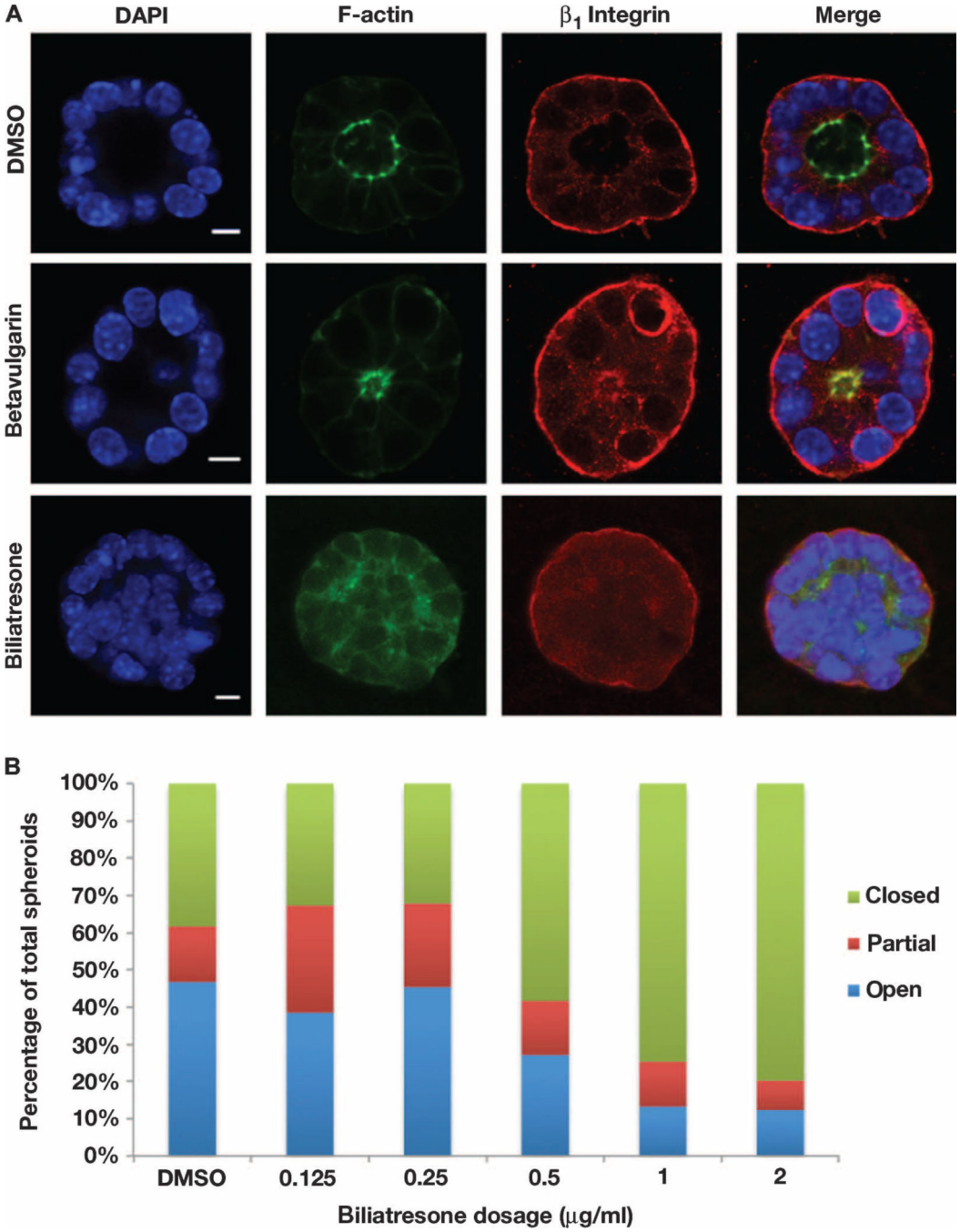

Fig. 5. Biliatresone-induced mouse cholangiocyte injury

(**A**) Confocal sections through cholangiocyte spheroids treated with vehicle, betavulgarin (2 μg/ml), or biliatresone (2 μg/ml) for 24 hours and stained with antibodies against F-actin or the β_1-integrin subunit, or with DAPI. The biliatresone-treated spheroid shows disruption of the spheroid lumen and abnormal cholangiocyte polarity, as evidenced by altered distribution of F-actin and by cholangiocyte stratification. Most betavulgarin-treated spheroids demonstrated decreased lumen size, but there was no loss of polarity or disruption of the monolayer (see fig. S17). Representative images from five independent experiments

are shown. DAPI, 4′,6-diamidino-2-phenylindole. (**B**) Dose-response experiment showing progressive increase in the percentage of abnormal biliatresone-treated spheroids beginning at 0.5 μg/ml. Scale bars, 7 μm. *n* = 48 to 89 spheroids counted per condition.